Last glacial-interglacial productivity and associated changes in the eastern Arabian Sea

D.K. Naik [a,*], Rajeev Saraswat [a], David W. Lea [b], S.R. Kurtarkar [a], A. Mackensen [c]

[a] Micropaleontology Laboratory, Geological Oceanography Division, National Institute of Oceanography, Goa, India
[b] Department of Earth Science, University of California, Santa Barbara 93106-9630, USA
[c] Alfred Wegner Institute for Polar and Marine Research, Bremerhaven, Germany

ABSTRACT

We reconstruct paleo-productivity and bottom water oxygenation changes during the past 32 ka, from the southeastern Arabian Sea, using absolute abundance of planktic foraminifera, relative abundance of Globigerina bulloides, angular asymmetrical benthic foraminifera (AABF), measurements of total organic carbon (C_{org}), %$CaCO_3$, and Globigerinoides ruber $\delta^{18}O$ and $\delta^{13}C$. The faunal and geochemical proxies suggest that productivity in the southeastern Arabian Sea was high during MIS 3. A distinct decrease in productivity is inferred during the last glacial maximum (19–23 ka) (LGM). Bottom water was well oxygenated during MIS3, only to become oxygen-depleted during the LGM. Productivity decreased abruptly during Heinrich Stadial 1 (HS-1), but the response to Heinrich Stadial 2 (HS-2) was different. Low productivity during the early deglaciation is also synchronous with an increase in ice-volume corrected $\delta^{18}O$ ($\delta^{18}O_{sw-ivc}$), a salinity proxy, between 18.9 (18.3–18.9) ka BP and 15.9 (15.0–16.3) ka BP, and a concomitant decrease in $\delta^{13}C$ between 18.2 (17.5–18.7) ka BP and 16.4 (15.3–16.7) ka BP. These patterns suggest that the global $\delta^{13}C$ minimum event during the last deglaciation was associated with the weak monsoon interval during HS-1 and a drop in productivity in tropical regions. A progressive increase in productivity is observed throughout the Holocene, with a distinct jump at 5.4 (3.8–6.3) ka BP. We infer that although productivity was higher in the eastern Arabian Sea during most of the last glacial interval, the overall resultant carbon sequestration was confined only to a restricted zone and not large enough to substantially alter atmospheric CO_2.

© 2016 Published by Elsevier B.V.

1. Introduction

Glacial-interglacial transitions indicate a close relationship between deglacial warming and rising atmospheric CO_2 (Monnin et al., 2001; Shakun et al., 2012; Marcott et al., 2014). Temporal changes in marine productivity, especially in the Southern Ocean, have been proposed as one of the factors which drive glacial-interglacial change in atmospheric CO_2 (Martin, 1990; Martínez-Garcia et al., 2009; Jaccard et al., 2016). Although field and modeling studies supported those findings, they inferred that the Southern Ocean enhanced iron fertilization induced productivity changes during the glacial interval can account only for ~40 ppmv change out of the total 80–100 ppmv change in atmospheric CO_2 during the last glacial-interglacial transition (Archer et al., 2000; Watson et al., 2000; Kohfeld et al., 2005; Brovkin et al., 2012). Other regions with increased glacial productivity that might have contributed to the glacial atmospheric CO_2 drop are yet to be identified (Costa et al.,

2016). Contrasting records of marine productivity during the last glacial-interglacial transition, however, suggest that regional productivity changes are highly variable (Jaccard et al., 2013). The Arabian Sea is one of the most productive tropical regions at present (Banse, 1987; Marra and Barber, 2005). Even though a majority of the records from the summer monsoon-dominated western Arabian Sea suggest reduced primary production during the last glacial maximum (LGM) (Prell and Kutzbach, 1987; Naidu and Malmgren, 1996; Gupta et al., 2003, 2008), contrasting results have been obtained from the eastern Arabian Sea, where both the summer and winter monsoon influence primary productivity, necessitating a reassessment of past productivity changes in this region (Agnihotri et al., 2003; Bassinot et al., 2011; Gupta et al., 2011; Singh et al., 2011).

Productivity in the Arabian Sea is monsoon-dominated (Lévy et al., 2007), as indicated by the fact that during the monsoon season, the carbonate flux constitutes ~50–60% of the total flux to the sea floor (Fig. 1) (Nair et al., 1989). Calcification increases several-fold during the monsoon season compared to non-monsoon months (Balch et al., 2001). High chlorophyll-a concentrations, a surface productivity indicator, are reported towards the end of the northeast (February) and southwest

* Corresponding author.
  E-mail addresses: dineshkumarnaikdu@gmail.com (D.K. Naik), rsaraswat@nio.org
(R. Saraswat).

Table 1
The details of the cores discussed in the manuscript.

| Reference	Length (cm)	Longitude (°E)	Latitude (°N)	Water depth (m)	Core	Sr. no.
Ivanochko (2004)	na	72.57	15.53	1230	MD76-131	1
Banakar et al. (2005a)	410	72.85	15.48	2500	SK117 GC8	2
Singh et al. (2006)	473	72.97	15.25	840	SK17	3
Agnihotri et al. (2003)	150	71.70	12.80	1680	3104G	4
Kessarkar et al. (2010)	490	73.33	12.63	1940	SK126 GC39	5
Kessarkar et al. (2013)	508	74.61	11.50	800	AAS62 GC01	6
Saraswat et al. (2013)	286	75.00	10.98	1247	SK237 GC04	7
Narayana et al. (2009)	250	75.53	10.27	875	AAS38 GC5	8
Narayana et al. (2009)	270	75.65	10.25	240	AAS38 GC4	9
Sarkar et al. (1993)	na	71.83	10.00	2523	SK20-185	10
Guptha et al. (2005)	552	71.98	9.33	2300	SK129 CR05	11
Anil Kumar et al. (2005)	480	76.05	8.03	1420	SK126 GC16	12
Sirocko (2002)	1340	76.43	7.30	1254	MD77-191	13
Agnihotri et al. (2003)	150	74.00	6.00	2680	3101G	14
Cayre et al. (1999)	5400	73.87	5.06	2446	MD 900963	15

na: The exact length of the core is not available.

(August–September) monsoon (Banse, 1987; Marra and Barber, 2005). Various parts of the Arabian Sea, however, respond differently to the seasonal wind forcing, leading to a huge regional variation in productivity during different seasons (Wiggert et al., 2005) (Fig. 1). The winds associated with the summer monsoon, drive productivity via intense coastal upwelling, lateral advection of nutrient-rich upwelled water, and offshore Ekman pumping in the western Arabian Sea (Wyrtki, 1973; Lévy et al., 2007). Productivity in the northern and central Arabian Sea region is driven by intense convective mixing and deepening of the mixed layer during the winter monsoon (Madhupratap et al., 1996). Regional differences in surface productivity have also been inferred in the mesotrophic northern and oligotrophic eastern Arabian Sea, and comparatively weaker differences in productivity between glacial and interglacial intervals are observed in the eutrophic upwelling area off Oman in the western Arabian Sea (Ivanova et al., 2003). Modeling studies predict a large change in monsoon patterns in a warming world, suggesting a possible variation in productivity in the Arabian Sea (Christensen et al., 2007). The response to such monsoon-induced productivity changes will, however, be regional. Therefore, it is necessary to understand changes in productivity in various parts of the Arabian Sea during different climatic regimes, such as the LGM, deglaciation and Holocene. Additionally, the monsoon-induced productivity in the Arabian Sea has also been suggested to respond to high latitude climatic changes including abrupt Heinrich Stadials (Singh et al., 2006, 2011).

Changes in productivity during, longer time periods as well as the last glacial-interglacial transition and Holocene have been reconstructed from different parts of the Arabian Sea (Prell and Kutzbach, 1987; Naidu and Malmgren, 1996; Agnihotri et al., 2003; Gupta et al., 2003, 2008; Bassinot et al., 2011; Singh et al., 2011). Productivity changes suggest that the southwest monsoon was weaker during glacial episodes, whereas the winter monsoon was stronger (Banakar et al., 2005a; Anil Kumar et al., 2005; Singh et al., 2011; Saraswat et al., 2005; 2014). A majority of these inferences are based on changes in the relative abundance of the planktic foraminifer *Globigerina bulloides*, which thrives in productive regions (Prell and Kutzbach, 1987; Naidu and Malmgren, 1996; Gupta et al., 2003; Bassinot et al., 2011). The abundance of *G. bulloides*, however, responds differently to wind-forced productivity changes in various parts of the Arabian Sea (Bassinot et al., 2011). Post-depositional diagenetic alteration can also affect paleo-productivity estimated from faunal abundance. Therefore, it is valuable to have paleo-productivity reconstructions from other proxies, such as changes in calcium carbonate percentage (%CaCO$_3$) and organic carbon (%C$_{org}$) in sediments (Agnihotri et al., 2003; Anil Kumar et al., 2005; Singh et al., 2006, 2011; Naidu et al., 2014). There is evidence, however, that both %CaCO$_3$ and %C$_{org}$ can also respond to different factors, such as surface production, sedimentation rates, dilution and preservation, in various parts of the Arabian Sea (Calvert et al., 1995; Guptha et al., 2005). Here we reconstruct paleo-productivity and water column oxygenation changes in the southeastern Arabian Sea region during the past 32 ka using faunal and geochemical proxies, in order to understand the potential role of this region in regulating carbon cycle on glacial-interglacial time-scales. Additionally, we try to understand the possible physical forcing, that affected productivity in the southeastern Arabian Sea (SEAS) during the last glacial interval.
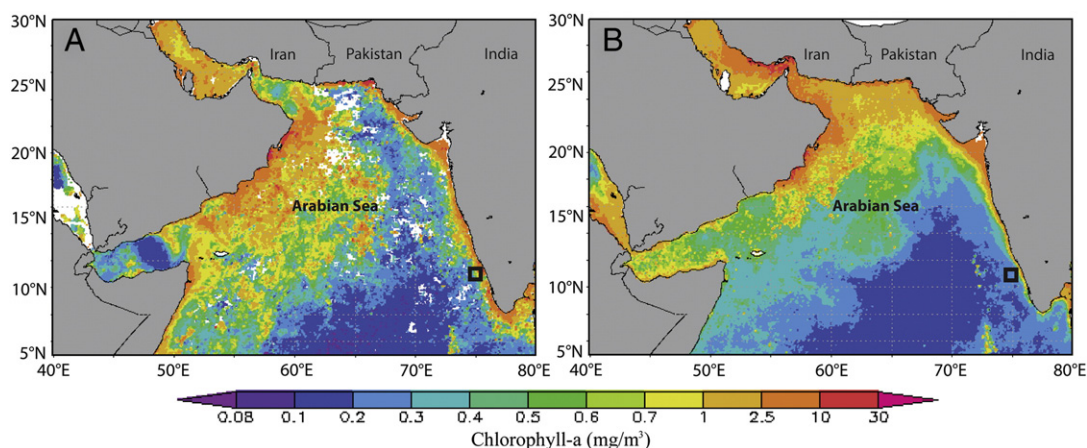
Fig. 1. Surface primary productivity (chlorophyll-a, mg/m^3) in the Arabian Sea during (A) the southwest (June–July–August–September) (B) and northeast (November–December–January–February) monsoon season (Acker and Leptoukh, 2007). The position of the Malabar core is marked with an open black square.

2. Oceanographic setting

The southeastern Arabian Sea is characterized by a seasonal reversal of surface currents in response to prevailing winds (Shankar et al., 2002). The equatorward West India Coastal Current brings relatively more saline water from the northern Arabian Sea to the SEAS prior to and during the southwest monsoon, whereas the poleward winter monsoon current transports low salinity water from the western Bay of Bengal into the SEAS during boreal winter (Prasanna Kumar et al., 2004). The sea surface temperature (SST) in the SEAS increases during the pre-summer monsoon season, leading to the development of a mini warm pool that peaks in April. The SEAS mini warm pool dissipates prior to the onset of summer monsoon precipitation, as a result of up-welling (Shenoi et al., 1999). Moderate to intense upwelling occurs in the SEAS during the summer monsoon season as a result of the complex interaction between alongshore wind stress, coastally trapped Kelvin waves, and the offshore propagating Rossby waves (Naidu et al., 1999; Lévy et al., 2007; Smitha et al., 2008). The upwelling causes a several-fold increase in productivity in the SEAS during summer monsoon season (Lévy et al., 2007). The region is also marked by a perennial inter-mediate water depth oxygen minimum zone (OMZ) which extends from ~150 m to ~1200 m (Naqvi, 1991; Naqvi et al., 2003). The Western Ghats, marking the eastern boundary of the SEAS, receive 2700 mm of rainfall during the summer monsoon, resulting in a large amount of sur-face runoff into the SEAS. The influence of the runoff extends, however, only to the inner shelf region (Chauhan et al., 2011).

3. Materials and methodology

Gravity core SK237 GC04, hereafter referred to as the Malabar core, was collected from 10°58.65′N latitude and 74°59.96′E longitude, at a water depth of 1245 m, towards the lower boundary of the perennial in-termediate depth OMZ (Saraswat et al., 2013) (Fig. 2). The core was sub-sampled at 1 cm interval, and the chronology of the core was established by Accelerator Mass Spectrometer radiocarbon dates taken from Saraswat et al. (2013). A total of 8 Accelerator Mass Spectrometer radiocarbon dates on mixed planktic foraminifera, measured at the Cen-ter for Applied Isotope Studies, The University of Georgia, USA and cali-brated by using marine dataset (Marine09, Reimer et al., 2009) and Calib6.0 version (Stuiver and Reimer, 1993), employing a reservoir cor-rection for the eastern Arabian Sea of 138 ± 64 years (Southon et al., 2002), were used to establish the chronology of the core (Fig. 3). The complete details of the age model and associated errors, given in this study in parentheses following the indicated age as the 95% confidence interval, are described in Saraswat et al. (2013).

In order to pick foraminifera, 10–15 g of the sediment was collected in pre-weighed petri-dishes and dried overnight at 50 °C. The dried sed-iment was weighed and soaked in de-ionized water for 24 h. The over-lying water was decanted and the sediments were wet-sieved through a 63 μm sieve. The coarse fraction (CF) (>63 μm) retained on the sieve was transferred to 25 ml glass beakers and dried overnight. The dried CF was weighed and carefully transferred to plastic vials. The coarse fraction percentage (%CF) was calculated by dividing the weight of dried coarse fraction by the weight of the total dry sediment, multiplied by hundred. Benthic foraminifera were picked from the CF and were grouped into angular asymmetrical (AABF) and rounded symmetrical morpho-groups following Nigam et al. (1992, 2007, 2009). For planktic foraminiferal studies, CF was dry sieved over 150 μm. The absolute abundance of planktic foraminifera was calculated in the >150 μm size fraction. To calculate the relative abundance of *Globigerina bulloides*, a minimum of 300 specimens of planktic foraminifera were picked from >150 μm fraction from each sample.

A small aliquot (2–3 g) of completely freeze-dried sediment was finely powdered for total carbon and inorganic carbon analysis. The total carbon (TC) was measured with a CNS analyzer, whereas inorganic carbon (TIC) was measured with a coulometer. The precision of TIC
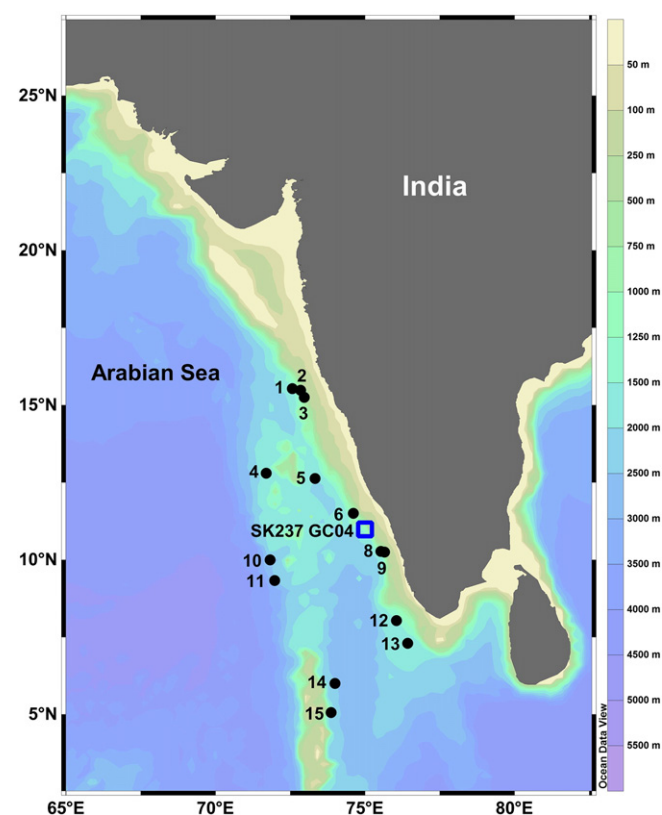
Fig. 2. Location of Malabar core SK237 GC04 is marked with a blue rectangle, whereas other cores discussed in the paper are plotted as filled circles: 1 - MD76–131, Ivanochko, 2004; 2 - SK117 GC8, Banakar et al., 2005a; 3 - SK17, Singh et al., 2006; 4 - 3104G, Agnihotri et al., 2003; 5 - SK126 GC39, Kessarkar et al., 2010; 6 - AAS62 GC01, Kessarkar et al., 2013; 8 - AAS38 GC5, 9 - AAS38 GC4, Narayana et al., 2009; 10 - SK20-185, Sarkar et al., 1993; 11 - SK129 CR05, Guptha et al., 2005; 12 - SK126 GC16, Anil Kumar et al., 2005; 13 - MD77-191, Sirocko, 2002; 14 - 3101G, Agnihotri et al., 2003; 15 - MD 900963, Cayre et al., 1999. The details of the cores are available in Table 1. The background is the bathymetry (plotted with Ocean Data View) with the scale on the right side of the map. (For interpretation of the references to color in this figure legend, the reader is referred to the web version of this article.)
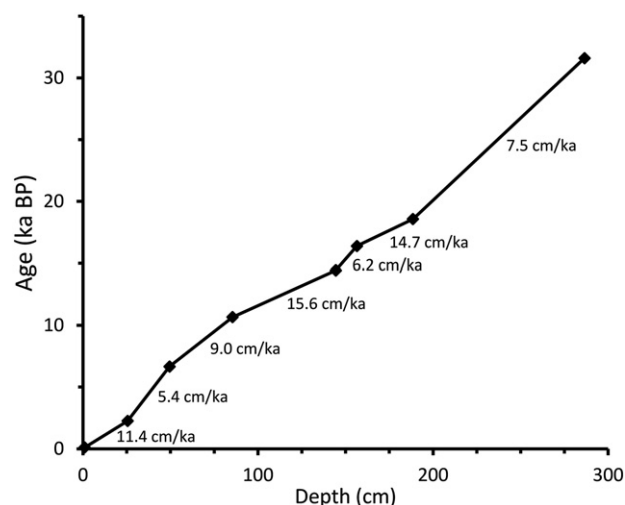
Fig. 3. Age model of the Malabar core, developed from 8 AMS radiocarbon dates (black symbols), measured on the mixed planktic foraminifera. The dates are plotted against the depth interval in the core and were used as tie points. Sedimentation rates between tie points are also shown. Further details of the age model are discussed in Saraswat et al. (2013).

measurements, based on repeat analysis of laboratory standard after every 10 samples, was better than ± 0.22%, whereas precision of TC measurements was better than ± 0.49%. Total organic carbon (C_{org}) was calculated by subtracting total inorganic carbon from the total carbon. The cumulative error associated with C_{org} estimates is ± 0.54%. The calcium-carbonate percentage (%$CaCO_3$) was calculated from the total inorganic carbon.

For stable carbon isotopic ratio ($\delta^{13}C$), 15–20 clean specimens of surface dwelling planktic foraminifer *Globigerinoides ruber* white variety, were picked from a narrow size range (250–355 μm) and analyzed by using a Finnigan MAT 251 isotope ratio gas mass spectrometer at the Alfred Wegener Institute for Polar and Marine Research, Bremerhaven, Germany. Precision of carbon isotope measurements based on repeat analyses of a laboratory standard over a one year period was better than 0.06‰. The ice-volume corrected $\delta^{18}O$ ($\delta^{18}O_{sw-ivc}$) was calculated by subtracting the ice-volume change caused by globally synchronous variation in seawater $\delta^{18}O$ (Waelbroeck et al., 2002) from $\delta^{18}O_{sw}$ reported in Saraswat et al. (2013). The resultant $\delta^{18}O_{sw-ivc}$ is a proxy for local evaporation/precipitation changes (Saraswat et al., 2012). Here we would like to note that the resultant $\delta^{18}O_{sw-ivc}$ may vary depending on the ice volume correction used to calculate $\delta^{18}O_{sw-ivc}$. In order to assess the difference in $\delta^{18}O_{sw-ivc}$ calculated by using different ice-volume corrections suggested for the last 32 ka, we used the ice-volume estimates reported by both Shackleton (2000) and Waelbroeck et al. (2002). Even though the actual estimates are slightly different, both estimates have a similar pattern. The difference in the two estimates is within the error limit. As the error associated with $\delta^{18}O_{sw}$ is ± 0.3‰ (Saraswat et al., 2013), it is assumed that the error in $\delta^{18}O_{sw-ivc}$ reported here, will be at least ± 0.3‰. Surface productivity maps were prepared by using the Giovanni online data system, developed and maintained by the NASA GES DISC (Acker and Leptoukh, 2007).

4. Results

The range of values in the Malabar core is from 4.5% to 32.5% for *G. bulloides* abundance, 1.5% to 5.4% for %C_{org}, 8.6% to 25.8% for %$CaCO_3$, 1.4% to 5.4% for %CF, 0.1‰ to 1.4‰ for $\delta^{18}O_{sw-ivc}$ and 0.56‰ to 1.70‰ for $\delta^{13}C$ (Fig. 4). The relative abundance of *G. bulloides* peaks at 23.9 (21.7–26.1) ka BP, just prior to the LGM, and then drops until 20.4 (19.2–21.8) ka BP, followed by an abrupt increase which peaks at 18.4 (17.9–18.8) ka BP, at the end of the LGM (Fig. 4A). The relative abundance of *G. bulloides* continuously decreases throughout the early deglaciation from 18.4 (17.9–18.8) ka BP onwards, until 14.3 (13.8–15.0) ka BP. The relative abundance of *G. bulloides* increases during the early Holocene until 5.4 (3.8–6.3) ka BP. The *G. bulloides* abundance is uniform throughout the last ~5 ka.

Malabar core %C_{org} was markedly lower during the last glacial interval prior to the beginning of deglaciation at ~18 ka BP, averaging 2.43 ± 0.26% versus 4.24 ± 0.75% during the late Holocene (last 5 ka) (Fig. 4B). The %C_{org} was somewhat higher during the LGM, as compared to the interval prior to the LGM. An abrupt decrease in %C_{org} is observed early in the deglacial transition, between 18.4 (17.7–18.7) and 14.3 (13.8–15.0) ka BP. A gradual increase in %C_{org} is observed throughout the Holocene, with minor fluctuations during the mid-Holocene (Fig. 4B).

An abrupt peak (44%) in %$CaCO_3$ is observed at 29.21 (27.1–30.8) ka BP, prior to the LGM, during the last glacial interval (Fig. 4C). A clear increase in %$CaCO_3$ occurs between 11.25 (8.8%) and 5.75 ka BP (24.7%). The temporal changes in total carbon are similar to those in %$CaCO_3$, except during the late Holocene, when total carbon increases rapidly (Fig. 4D). The temporal variations in %$CaCO_3$ also have some similarity to the changes in %CF (Fig. 4E). Depending upon its constituents, the CF% is closely linked to productivity, carbonate preservation or terrigenous influx. The planktic foraminiferal abundance gradually increases during the last glacial interval, prior to the LGM, and then decreases afterwards (Fig. 4F). The planktic foraminiferal abundance sharply decreases during the early deglaciation, similar to the changes in %CF. A gradual
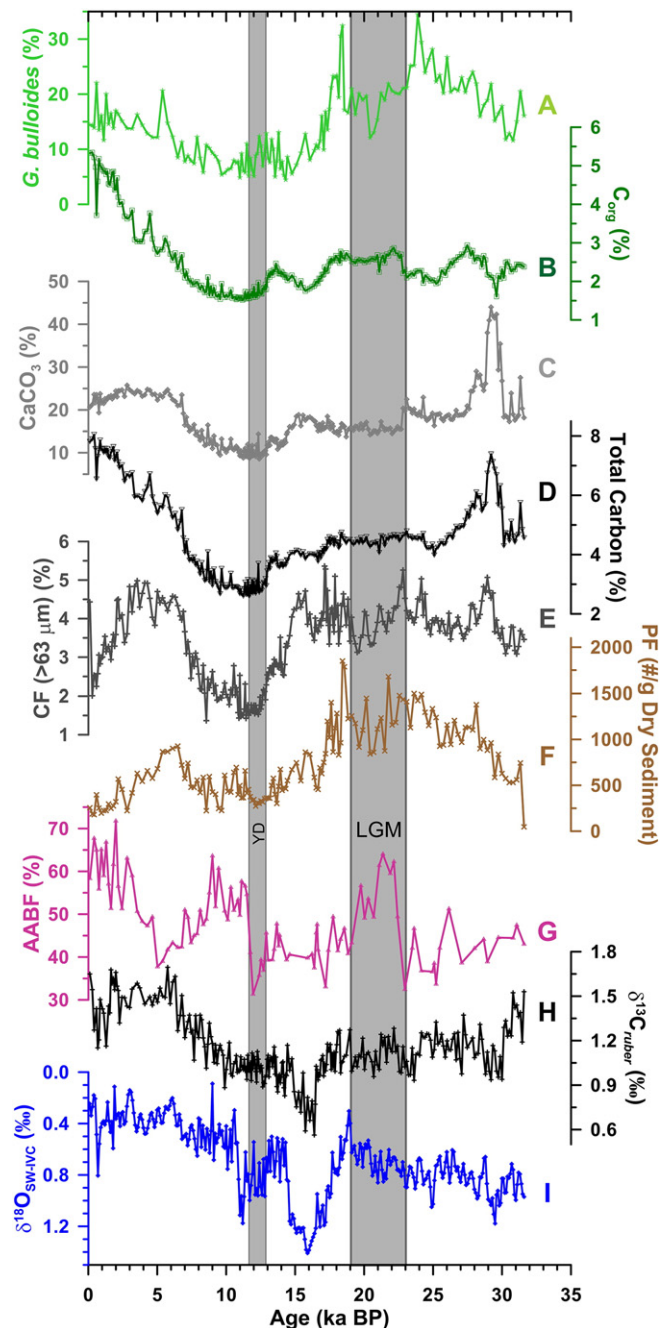
Fig. 4. Changes in faunal and geochemical parameters in the Malabar core during the last 32 ka. A. Relative abundance of planktic foraminifer *G. bulloides*, a proxy for upwelling induced primary productivity; B. Organic carbon weight percentage (%C_{org}); C. $CaCO_3$ weight percentage; D. Total carbon percentage in dry sediments; E. Percentage of coarse fraction (CF) (>63 μm); F. Abundance of all planktic foraminifera (PF) per gram dry sediment; G. Relative abundance of angular asymmetrical benthic foraminifera (%AABF), an indicator of bottom water oxygenation; H. $\delta^{13}C_{ruber}$; and I. Ice-volume corrected $\delta^{18}O$ ($\delta^{18}O_{sw-ivc}$), a proxy for local precipitation-evaporation. The gray shaded bars indicate the last glacial maximum and younger Dryas interval. The data used in this figure is available online as Supplementary Table 1.

increase in planktic foraminiferal abundance is observed during the early Holocene, peaking at 6.49 (5.95–6.77) ka BP, followed by a gradual decrease during the late Holocene. The %AABF was generally lower during the glacial interval prior to LGM (Fig. 4G). An abrupt increase in %AABF is, however, observed during the LGM, with a maximum at 21.36 (19.7–23.2) ka BP. Between the LGM and late Holocene, there are two clear maxima in %AABF, the first at 9.0 (7.9–10.1) ka and the second at 2.0 (1.5–2.3) ka.

The $\delta^{13}C$ of *G. ruber* was depleted during the last glacial interval, averaging $1.08 \pm 0.15‰$, as compared to $1.31 \pm 0.21‰$ in the Holocene (Fig. 4H). A very clear minimum in $\delta^{13}C$ reaching 0.56‰ occurs during the deglaciation and coincides with Heinrich Stadial 1 (HS-1). The $\delta^{13}C$ increases steadily throughout the early Holocene until the mid-Holocene [5.75 (4.13–6.55) ka BP]. The $\delta^{18}O_{sw-ivc}$ was enriched during the last glacial interval, as compared to the Holocene (Fig. 4I). A marked maximum in $\delta^{18}O_{sw-ivc}$ is evident during the early deglaciation, reaching 1.4‰ value at 15.9 (14.9–16.3) ka BP, coincident with the minimum in $\delta^{13}C$. A less marked maximum is observed at 11.2 (10.7–11.1) ka BP. The $\delta^{18}O_{sw-ivc}$ was slightly more negative, averaging $0.48 \pm 0.12‰$, during the early Holocene, compared to the glacial interval ($0.83 \pm 0.21‰$) (Saraswat et al., 2013).

5. Discussion

5.1. Last glacial interval

High *G. bulloides* abundance during the last glacial interval, combined with a similar higher absolute abundance of planktic foraminifera, %CaCO$_3$, %TC, as well as high %CF (dominated by foraminiferal tests, pteropod shells and its fragments), suggests increased productivity during the glacial interval. Most of this more productive interval coincides with depleted $\delta^{18}O_{sw-ivc}$. During the LGM, *G. bulloides* abundance actually decreased, as compared to the prior interval, accompanied by a drop in %CaCO$_3$, %CF, and planktic foraminiferal number, suggesting decreased productivity in the SEAS (Agnihotri et al., 2003). LGM productivity was, however, still higher than during the deglaciation and Holocene.

High *G. bulloides* flux has earlier been reported from high productivity regions (Naidu et al., 1992; Conan and Brummer, 2000), and temporal changes in its flux have been utilized as a proxy to reconstruct productivity changes (Naidu and Malmgren, 1996; Zaric et al., 2005). The possible post-depositional alteration of planktic foraminiferal assemblages, and thus the relative abundance of *G. bulloides*, is unlikely because the core lies well above the foraminiferal lysocline (Cullen and Prell, 1984). Further, dissolution-susceptible planktic foraminiferal species are well preserved all along the western continental margin of India, suggesting negligible carbonate dissolution (Naidu et al., 1992). Therefore, the planktic foraminiferal assemblage in the sediments at the Malabar site likely reflect the living assemblage, even though the final settling flux might be only a fraction of the total initial production (Conan et al., 2002). The application of %CaCO$_3$ to reconstruct past productivity changes in the eastern Arabian Sea stems from the observation that substantially increased biogenic carbonate flux is associated with times of higher surface productivity (Nair et al., 1989; Sirocko et al., 1993; Balch et al., 2001). Temporal changes in %CaCO$_3$, however, are also influenced by changes in terrigenous input/dilution (Naidu et al., 1992; Agnihotri et al., 2003).

Interestingly, high *G. bulloides* abundance, suggesting enhanced productivity during the last glacial interval, is not always accompanied by a corresponding increase in %C$_{org}$. Between 28 and 25 ka BP, constant *G. bulloides* relative abundances coincide with a clear net drop in %C$_{org}$. This interval is marked by a net decrease in total carbon as well as CaCO$_3$. The abrupt drop in *G. bulloides* relative abundance during the LGM is accompanied by a small increase in %C$_{org}$. Naidu et al. (1992) and Calvert et al. (1995) inferred that C$_{org}$ accumulation in the sediments can be used as an indicator of past productivity changes. Decoupling between *G. bulloides* abundance and %C$_{org}$, in the Malabar core, however, points towards factors other than productivity affecting C$_{org}$ accumulation in sediments. Canfield (1994) proposed that in marine sediments deposited with sedimentation rates below 40 cm/ka, enhanced preservation of C$_{org}$ may be found under low bottom water dissolved oxygen conditions. The drop in %C$_{org}$ between 28 and 25 ka BP is marked by low %AABF, suggesting well ventilated bottom water and thus poor organic matter preservation (Nigam et al., 2007;

Mazumder and Nigam, 2014). The increase in %C$_{org}$ during the LGM corresponds with an increase in %AABF, suggesting poorly ventilated waters (Singh et al., 2015) and thus better preservation of organic carbon, although this relationship is not consistent during all time intervals. In contrast, redox-sensitive elements (Cr and V) suggest no significant change in bottom water anoxia during the LGM (Agnihotri et al., 2003). Additional differences in productivity inferred from the relative abundance of *G. bulloides* and %C$_{org}$ might also be related to the influence of sedimentation rate on %C$_{org}$ (Agnihotri et al., 2003). The %C$_{org}$ in a few cores collected from the eastern Arabian Sea did significantly increase during the LGM and was attributed to an increase in sedimentation rates leading to better C$_{org}$ preservation during the LGM (Agnihotri et al., 2003).

High productivity during the last glacial interval has also been reported in other cores collected from the eastern Arabian Sea. Anil Kumar et al. (2005) inferred enhanced surface productivity in the eastern Arabian Sea during the last glacial period from increased %C$_{org}$ and %CaCO$_3$. Banakar et al. (2005a) also suggested increased productivity during the glacial interval coupled with weaker water column denitrification. In another core (MD77194), collected from north (10°28′N, 75°14′E) of the SEAS from a similar water depth (1222 m), substantially increased primary productivity was inferred during the last glacial interval, by using foraminiferal transfer functions (Cayre and Bard, 1999). In all of these studies, high glacial productivity has been attributed to strengthened winter monsoon leading to enhanced convective mixing (Anil Kumar et al., 2005; Banakar et al., 2005a; Dahl and Oppo, 2006; Singh et al., 2006, 2011; Anand et al., 2008). A similar mechanism is unlikely to have enhanced productivity in the southeastern Arabian Sea, because a substantial increase in productivity in the southeastern Arabian Sea is observed only during the southwest monsoon season (Lévy et al., 2007). The increased productivity in this region is remotely forced by the stronger upwelling-favorable winds in the Bay of Bengal (BoB) (Shankar and Shetye, 1997), thus suggesting a strong influence of the physical state of the BoB on upwelling in this area. The onset of increasing productivity in the Lakshadweep Sea region, however, lags that in the coastal regions by a couple of months (Lévy et al., 2007). The upwelling that causes high productivity in the Lakshadweep Sea region is remotely forced by Rossby waves radiating westward off the Indian coast, thus resulting in a lag in productivity compared to that in the shallow water regions off the west coast of India (Shankar and Shetye, 1997; Shankar et al., 2004). The peak summer monsoon productivity in the shallow water regions off the west coast of India is synchronous with that in the Lakshadweep Sea region (Lévy et al., 2007). A similar physical forcing is unlikely to operate during the glacial interval because sea level was ~120 m lower (Siddall et al., 2003) and the entire modern continental shelf was exposed. These changes might have caused higher productivity during the glacial interval because of the direct input of the riverine influx closer to the Malabar core region, unlike at present, when it is confined only to the shallow shelf (Chauhan et al., 2011). Although the summer season upwelling might have diminished during the glacial interval as a result of weaker summer winds, the proximity of terrigenous input and a possible lack of lag in upwelling, due to the reduced distance between the then coastal region and core location, which lies in the continental slope, might have supported higher glacial productivity in the SEAS. Another factor that might have increased productivity in the SEAS is the weaker stratification as a result of reduced influx of low salinity Bay of Bengal water (Mahesh and Banakar, 2014). The pre-summer monsoon stratification in this region is driven by influx of low salinity Bay of Bengal water as it acts as a prominent barrier layer (Shenoi et al., 1999). Reduced influx of low salinity Bay of Bengal water during the glacial interval (Mahesh and Banakar, 2014), was thus possibly responsible for the increased productivity in this region. The reduced influx of low salinity water during the glacial interval is further supported by consistently low Ba/Ca ratio in planktic foraminifer *G. ruber* (Saraswat et al., 2013). Additionally, even if the influx continued, as is inferred by Sarkar et al. (1990), it would not have caused

strong stratification as its salinity would have been higher due to reduced freshening of the Bay during the weaker glacial summer monsoon regime (Mahesh and Banakar, 2014). The southward shift in the inter-tropical convergence zone in the Northern Hemisphere during the glacial interval (Broccoli et al., 2006) would have also helped promote high productivity due to reduced cloud cover, because high cloud cover is one of the factors responsible for low primary productivity in the northern Bay of Bengal at present (Prasanna Kumar et al., 2002).

The drop in productivity during the LGM is intriguing. A repeated abrupt decrease in *G. bulloides* on millennial time-scales during cold intervals was also reported from the central eastern Arabian Sea and attributed to reduced winter monsoon strength resulting in strong stratification as witnessed during the inter-monsoon months at present (Singh et al., 2011). At the Malabar core site also, the LGM productivity collapse is attributed to stronger stratification. The cause of stronger stratification at this core site was likely due to a weaker summer monsoon coupled with enhanced transport of low salinity Bay of Bengal water, as evident from a consistently depleting $\delta^{18}O_{sw-ivc}$ throughout the LGM (Fig. 4I). The enhanced transport of low salinity Bay of Bengal water is further supported by an increase in *G. ruber* Ba/Ca ratio during this interval (Saraswat et al., 2013).

5.2. The deglaciation

A large decrease in *G. bulloides* relative abundance with a corresponding decrease in planktic foraminiferal abundance as well as %C$_{org}$ suggests a decrease in surface productivity during the deglaciation, in contrast to paleoproductivity changes estimated from other low- and mid-latitude upwelling areas (Agnihotri et al., 2003). The early deglaciation is also marked by significantly enriched $\delta^{18}O_{sw-ivc}$, suggesting reduced precipitation, which is consistent with the reduced primary productivity as inferred from relative abundance of *G. bulloides*. The early deglacial enriched $\delta^{18}O_{sw-ivc}$ combined with reduced Ba/Ca ratio during this interval (Saraswat et al., 2013), does not support an early deglacial strengthening of winter monsoon as suggested earlier (Tiwari et al., 2005). The early deglaciation is also marked by a decrease in %AABF, suggesting well-ventilated bottom water and thus poor C$_{org}$ preservation. Minimum surface productivity during the early deglaciation, as a result of a weaker southwest monsoon, has also been reported from several parts of the eastern Arabian Sea (Sirocko et al., 1993, 2000; Cayre and Bard, 1999; Singh et al., 2006). The %CF and %CaCO$_3$ in the Malabar core, however, are constant during the early deglaciation until 15.3 (14.5–15.9) ka BP, suggesting better preservation of biogenic carbonates during this time interval.

A small but net increase in *G. bulloides* relative abundance is observed during the Younger Dryas (YD) chronozone (Fig. 4B). The %C$_{org}$, %CaCO3, %CF, and planktic foraminiferal abundance were, however, low during the YD. This interval is also marked by enriched $\delta^{18}O_{sw-ivc}$, suggesting either weaker monsoon or reduced influx of low saline Bay of Bengal water. A concomitant decrease in Ba/Ca ratio during this interval (Saraswat et al., 2013) further confirms decreased surface runoff and thus enriched $\delta^{18}O_{sw-ivc}$. The %C$_{org}$ during the YD was low despite increased bottom water dissolved oxygen as inferred from a drop in %AABF. Deglacial rise in sea level, coupled with further weakened summer monsoon (Saraswat et al., 2013), would have reduced the nutrient supply to the deeper regions and thus caused reduced productivity during the glacial termination, as inferred from the drop in relative abundance of *G. bulloides*, %CF as well as planktic foraminiferal abundance.

5.3. Early Holocene

The relative abundance of *G. bulloides*, planktic foraminiferal abundance and %C$_{org}$ decreased for a brief time during the early Holocene, between 11.12 and 8.56 ka BP, suggesting a short phase of low productivity. The low productivity during the early Holocene is attributed to enhanced fresh water influx due to a stronger summer monsoon (Sirocko et al., 2000), or enhanced transport of low saline water from the Bay of Bengal. The fresh water would have lead to a low salinity cap resulting in reduced surface productivity (Kessarkar and Rao, 2007), as inferred from an abrupt shift from highly enriched to depleted $\delta^{18}O_{sw-ivc}$, as compared to the deglaciation. A decrease in %C$_{org}$ and %CaCO$_3$ during the early Holocene in a few other cores collected from the SEAS was also attributed to intense southwest monsoon induced decrease in surface productivity due to fresh water influx (Agnihotri et al., 2003; Anil Kumar et al., 2005). The %AABF is very high during the early Holocene, suggesting the presence of an intense OMZ, as a result of reduced ventilation.

The brief early Holocene low productivity interval was followed by a phase of consistently increasing productivity, until the mid-Holocene as inferred from a gradual increase in *G. bulloides*, planktic foraminiferal abundance and %C$_{org}$ (Bassinot et al., 2011). Following the minor enrichment of $\delta^{18}O_{sw-ivc}$ for a brief interval during the late deglaciation and early Holocene, an abrupt shift in $\delta^{18}O_{sw-ivc}$ towards more depleted values is observed at ~10.6 (10.5–10.9) ka BP, which is followed by a further gradual depletion until the mid-Holocene, suggesting increased precipitation. This interval of gradually increasing surface productivity is marked by a large decrease in %AABF, until the mid-Holocene, suggesting well ventilated waters. The %CF as well as %CaCO$_3$ also increase during the early Holocene, suggesting either better preservation or a decrease in terrigenous input. The mid-Holocene peak in *G. bulloides* abundance, attributed to higher productivity, is accompanied by an increase in planktic foraminiferal abundance, as well as %CF and %CaCO$_3$. A very low %AABF during the mid-Holocene confirms increased availability of dissolved oxygen in bottom waters, which might have resulted in better preservation of CaCO$_3$.

5.4. Late Holocene

The relative abundance of *G. bulloides* increases steadily during the early Holocene, suggesting a concomitant increase in productivity of the eastern Arabian Sea (Singh et al., 2006). The abundance of *G. bulloides* is, however, relatively unchanged during the last 5 ka, suggesting no major change in surface productivity. The %CaCO$_3$ also remained relatively constant during the last 5.8 (4.1–6.5) ka. In contrast, small fluctuations with a net enrichment of $\delta^{18}O_{sw-ivc}$ between 3 ka BP and 0.8 ka BP are observed, suggesting reduced precipitation during the late Holocene. The reduced precipitation is accompanied by a decrease in both the planktic foraminiferal abundance as well as %CF. Over the same time interval, %AABF as well as %C$_{org}$ increase, both reaching maxima in the youngest interval, suggesting an intensification of the OMZ in the latest Holocene due to restricted ventilation of bottom water. These findings are supported by increased denitrification during the late Holocene, which was previously attributed to less oxygenated waters (Kessarkar et al., 2010; Naik et al., 2014). The decrease in %CF and planktic foraminiferal abundance observed in the Malabar core is attributed to increased dissolution/fragmentation of biogenic carbonates as a result of supralysoclinal dissolution. Supralysoclinal dissolution has also been suggested as the factor responsible for dissolution of biogenic carbonates during the Late Holocene in the eastern Arabian Sea (Kessarkar and Rao, 2007). The restricted detrital influx and confinement of terrigenous influx to the inner shelf, as sea-level reached its present position at ~5.7 ka, might have also contributed towards high %C$_{org}$ and %CaCO$_3$ during the late Holocene by reducing terrigenous dilution (Hashimi et al., 1995; Anil Kumar et al., 2005; Pattan et al., 2005).

The gradual increase in productivity throughout the Holocene, as inferred from the increase in relative abundance of *G. bulloides* (Fig. 7), is attributed to the strengthened summer monsoon winds in the SEAS, as a result of the southward shift of regional circulation patterns over the Indian Ocean (Bassinot et al., 2011). The Holocene monsoon evolution pattern in Malabar core is opposite to that reported from the Oman

margin, where proxy records including *G. bulloides* abundance suggest progressive weakening of the summer monsoon. This difference is attributed to the differential response of summer winds in these two regions (Bassinot et al., 2011). The precise physical forcing leading to increased glacial productivity in this region, however, can only be discerned by modeling the glacial circulation, which is outside of the scope of this paper.

5.5. Regional productivity changes

G. bulloides relative abundance-based paleoproductivity records of the late Quaternary from the eastern Arabian Sea are limited (a total of five records, including our record) and one of them only covers the Holocene (Singh et al., 2006, 2011; Bassinot et al., 2011; Gupta et al., 2011). Both the range of *G. bulloides* relative abundance and its temporal variation during the last 32 ka in the Malabar core is similar to records from cores collected from central eastern Arabian Sea on the lower slope region (SK17 - Singh et al., 2006; MD76-131 - Singh et al., 2011). The relative abundance of *G. bulloides* in the Holocene section of the Malabar core is also similar to that of core MD77-191, collected from the southeastern Arabian Sea, off the southern tip of India (Bassinot et al., 2011).

In contrast to the *G. bulloides* relative abundance, a comparison of the Malabar records with other cores from the eastern Arabian Sea suggests divergent patterns in both %$CaCO_3$ (Fig. 5) and %C_{org} (Fig. 6) accumulation over the last 32 ka. Changes in %$CaCO_3$ and %C_{org} in cores collected within the OMZ and outside the OMZ also diverge over the last 32 ka. Cores collected from the modern day lower boundary (1250 to 1500 m, Naqvi et al., 2003) of the OMZ, (i.e. Malabar core and MD76-131), show similar %$CaCO_3$ and %C_{org} values, as well as comparable patterns, throughout the last 32 ka. The *G. bulloides* relative abundance, as well as the %C_{org} in the Malabar core, also agrees with that in core SK17 collected from the north of SEAS at a water depth of 840 m (Singh et al., 2006). High C_{org} values during the Late Holocene are observed only in the Malabar core and core AAS38-GC5. Increases in %$CaCO_3$ abundance during the late Holocene, as compared to the LGM and termination, are also noted in a majority of the other cores. The absolute values and pattern of %C_{org} as well as %$CaCO_3$ in the Malabar core are also comparable with records from MD76–131 (Ivanochko, 2004) SK126 GC39 (Kessarkar et al., 2010) and AAS62/1 (Kessarkar et al., 2013), all collected from the lower continental slope. The differences in %$CaCO_3$ and %C_{org} values in cores collected from the eastern Arabian Sea are attributed to the fact that both of these parameters are highly susceptible to post depositional diagenetic changes. Detailed comparison thus suggests that the patterns in the Malabar core agree only with other cores collected from a comparable depth; the observed changes thus reflect a regional pattern marked by similar preservation conditions during deglaciation in the southeastern Arabian Sea.

5.6. Global teleconnections and implications

Productivity in the eastern Arabian Sea decreased abruptly during Heinrich Stadial 1 (HS-1) (Heinrich, 1988; Bond et al., 1997; Barker et al., 2009), as inferred from the drop in relative abundance of *G. bulloides* and supported by a matching decrease in %CF and planktic foraminiferal number. The response to Heinrich Stadial 2 (HS-2), was, however, different (Fig. 7). The relative abundance of *G. bulloides*, %CF and planktic foraminiferal number increased during HS-2, suggesting enhanced productivity. A drop in %C_{org} is, however, observed during both HS-1 and HS-2. Planktic $\delta^{13}C$ was also depleted during both HS-2 and HS-1: by 0.31‰ in HS-2, from 1.24‰ at 25.62 (23.2–27.8) ka BP to 0.93‰ at 23.62 (21.4–25.7) ka BP, and by 0.57‰ in HS-1, from 1.17‰ at 17.5 (16.6–18.2) ka BP to 0.6‰ at 16.4 (15.3–16.7) ka BP. The drop in $\delta^{13}C$ during HS-1 in the Malabar core is comparable with previous records from the Indian Ocean (Martinson et al., 1987; Banakar, 2005b; Raza and Ahmad, 2013). The contrasting response of productivity in
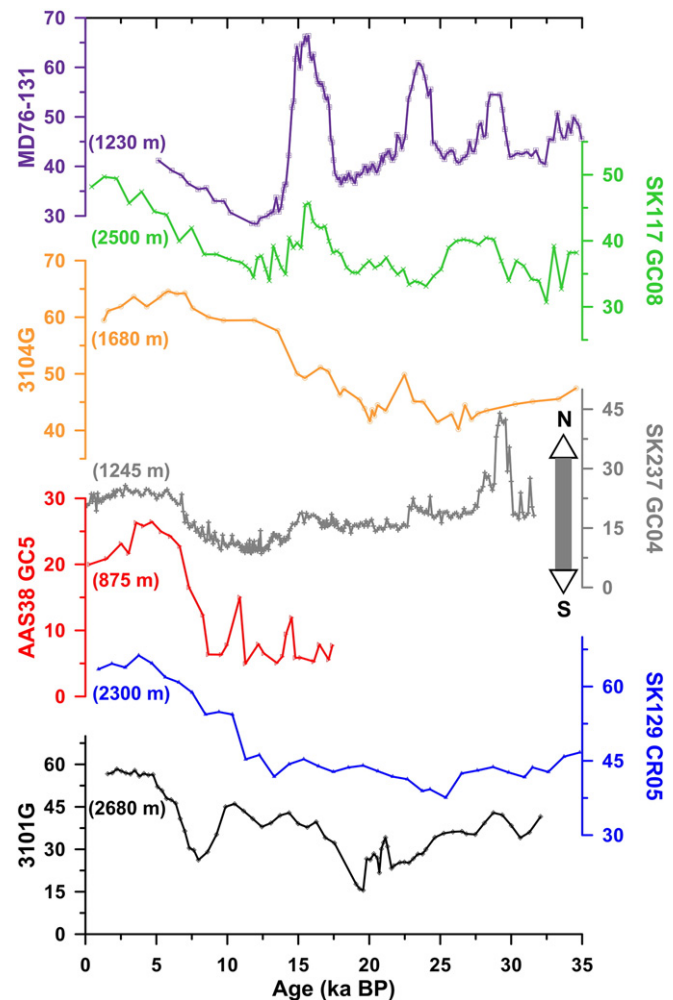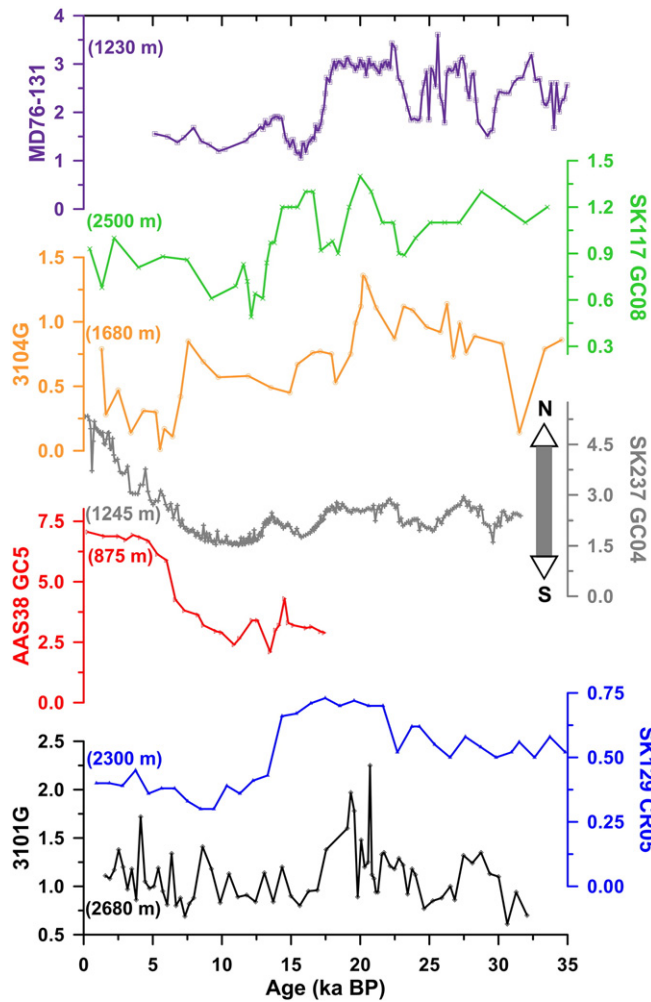

Fig. 5. Compilation of $CaCO_3$ (%) changes during the last 35 ka in different cores collected from the eastern Arabian Sea. The cores are plotted with the northernmost core on the top and the southernmost on the bottom. The water depth of the core is given in parenthesis, next to each record. For details of each core, refer to Fig. 2, and Table 1.

the SEAS to Heinrich Stadial events suggests a variable relationship between the SEAS and the North Atlantic, mediated through either oceanic circulation links (Alvarez-Solas et al., 2013) or atmospheric teleconnections. Another factor that might have contributed to the differential response of productivity in the SEAS to HS1 and HS2 is the difference in sea level during these two events. The rapid sea-level rise during the deglaciation increased the distance of the core site from the Western Ghats. The increased distance from the Western Ghats resulted in reduced terrigenous input to the core site (Chauhan et al., 2011) and thus reduced productivity. The drop in productivity during the early deglaciation was accompanied by a concomitant 1.1‰ increase in $\delta^{18}O_{sw-ivc}$, from 0.3‰ at 18.9 (18.3–18.9) ka BP to 1.4‰ at 15.9 (15.0–16.3) ka BP, suggesting that the decrease in productivity during the early deglaciation was associated with a monsoon-driven increase in E/P.

The Malabar core is characterized by a very well-defined *G. ruber* $\delta^{13}C$ minimum, falling from >1‰ (1.0 ± 0.06‰, prior to the minimum and 1.04 ± 0.09‰, after the minimum) to 0.76 ± 0.12‰ between 16.5 (16.8–15.5) and 14.9 (15.4–14.4) ka BP, with the most negative $\delta^{13}C$ values occurring between 16.4 (16.7–15.3) and 15.7 (16.2–14.9) ka BP (Fig. 7). This minimum is synchronous with the global $\delta^{13}C$ minimum dated at 15.9 ± 0.2 ka BP in tropical ocean sediments (Spero and Lea, 2002) and which is also apparent between 16 and 12 ka BP in ice core CO_2 (Schmitt et al., 2012; Bauska et al., 2016). By matching the minimum in Malabar $\delta^{18}O_{sw-ivc}$ to a likely coincident minimum in the absolute dated Hulu Cave speleothem record (Southon et al., 2012),
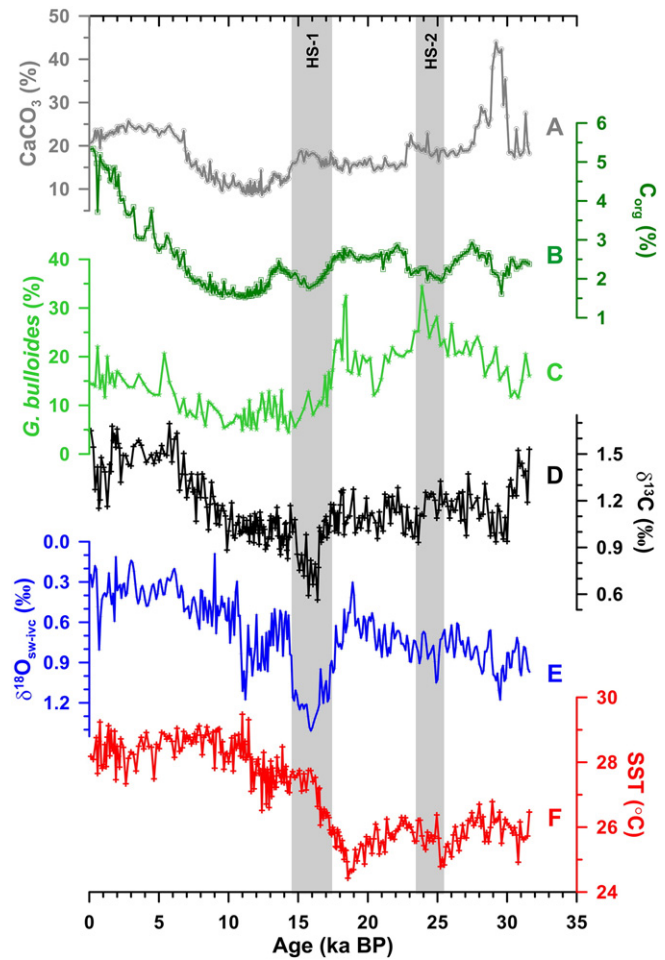
Fig. 6. Compilation of %C_{org} changes during the last 35 ka in different cores collected from the southeastern Arabian Sea. The cores are plotted with the northernmost core on the top and the southernmost on the bottom. The water depth of the core is given in parenthesis, next to each record. For details of the core, refer to Fig. 2, and Table 1.

Fig. 7. All productivity/monsoon proxy indicators analyzed in the Malabar core, along with the SST record from Saraswat et al., (2013): A - %$CaCO_3$; B - %C_{org}; C - Relative abundance of *G. bulloides*; D - $\delta^{13}C$; E - $\delta^{18}O_{sw-ivc}$. The SST change during the same interval is also plotted (F) (Saraswat et al., 2013). The vertical gray shaded region indicates Heinrich Stadials marked as HS-1 and HS-2. The %C_{org} as well as $\delta^{13}C$ in the SEAS decreases during high latitude Heinrich Stadials. The HS are also marked by an increase in $\delta^{18}O_{sw-ivc}$. A similarly consistent response is, however, not observed in %*G. bulloides*-based productivity changes.

we can further narrow the timing of the Malabar $\delta^{13}C$ minimum to 16.0 ka BP. The $\delta^{13}C$ minimum also coincides precisely with the end of the first and most rapid phase of deglacial Malabar SST rise, likely reflecting the end of the first rapid rise of atmospheric-CO_2 at 16.2 ka BP (Saraswat et al., 2013; Marcott et al., 2014) (Fig. 7). Based on the co-incident decrease in productivity during HS-1, which is very clear in the Malabar C_{org} record, and an increase in evaporation/precipitation in the southeastern Arabian Sea, we hypothesize that the global $\delta^{13}C$ minimum during the deglaciation was associated with a weak monsoon interval (Cheng et al., 2009; Saraswat et al., 2013; Tierney et al., 2016) and a drop in productivity in tropical regions.

6. Conclusions

Productivity and bottom water oxygenation changes during the past 32 ka reconstructed from the Malabar core from the southeastern Arabian Sea suggest that productivity in the southeastern Arabian Sea was high, with well-oxygenated waters during MIS 3. The LGM is characterized by an abrupt decrease in productivity, with oxygen-depleted waters. The contrasting response of productivity in the SEAS to Heinrich Stadial events 1 and 2 suggests a variable relationship between the SEAS and the North Atlantic, mediated through either oceanic circulation links or atmospheric teleconnections. A concomitant 1.1‰ drop in $\delta^{18}O_{sw-ivc}$ and 0.7‰ drop in $\delta^{13}C$ during HS-1 suggests that the

productivity decrease during the early deglaciation was associated with monsoon driven local evaporation-precipitation changes as well as the well-established global $\delta^{13}C$ minimum at 16 ka BP. A progressive increase in productivity is observed throughout the Holocene. The high glacial productivity as noted in the Malabar core as well as a few other cores collected from similar water depths is not observed in all the cores collected from the southeastern Arabian Sea. This observation suggests that although productivity was higher in this region during glacial episodes, the overall resultant carbon sequestration was confined only to a restricted zone and unlikely to substantially alter atmospheric CO_2.

Appendix A. Supplementary data

Supplementary data to this article can be found online at http://dx.doi.org/10.1016/j.palaeo.2016.07.014.

References

Acker, J.G., Leptoukh, G., 2007. Online analysis enhances use of NASA earth science data. Eos. Trans. AGU 88, 14–17.

Agnihotri, R., Sarin, M.M., Somayajulu, B.L.K., Bull, A.J.T., Burr, G.S., 2003. Late-quaternary biogenic productivity and organic carbon deposition in the eastern Arabian Sea. Palaeogeogr. Palaeoclimatol. Palaeoecol. 197, 43–60.

Alvarez-Solas, J., Robinson, A., Montoya, M., Ritz, C., 2013. Iceberg discharges of the last glacial period driven by oceanic circulation changes. Proc. Natl. Acad. Sci. 110, 16350–16354.

Anand, P., Kroon, D., Singh, A.D., Ganeshram, R.S., Ganssen, G., Elderfield, H., 2008. Coupled sea surface temperature–seawater $\delta^{18}O$ reconstructions in the Arabian Sea at the millennial scale for the last 35 ka. Paleoceanography 23, PA4207. http://dx.doi.org/10.1029/2007PA001564.

Anil Kumar, A., Rao, V.P., Patil, S.K., Kessarkar, P.M., Thamban, M., 2005. Rock magnetic records of the sediments of the eastern Arabian Sea: evidence for late Quaternary climatic change. Mar. Geol. 220, 59–82.

Archer, D., Winguth, A., Lea, D., Mahowald, N., 2000. What caused the glacial/interglacial atmospheric pCO2 cycles? Rev. Geophys. 38, 159–189.

Balch, W.M., Drapeau, D.T., Fritz, J., 2001. Monsoonal forcing of calcification in the Arabian Sea. Deep-Sea Res. 47, 1301–1337.

Banakar, V.K., Oba, T., Chodankar, A.R., Kuramoto, T., Yamamoto, M., Minagawa, M., 2005a. Monsoon related changes in sea surface productivity and water column denitrification in the eastern Arabian Sea during the last glacial cycle. Mar. Geol. 219, 99–108.

Banakar, V.K., 2005b. $\delta^{13}C$ depleted oceans before the termination 2: more nutrient-rich deep-water formation or light-carbon transfer? Indian J. Mar. Sci. 34, 249–258.

Banse, K., 1987. Seasonality of phytoplankton chlorophyll in the central and northern Arabian Sea. Deep-Sea Res. 34, 713–723.

Barker, S., Diz, P., Vautravers, M.J., Pike, J., Knorr, G., Hall, I.R., Broecker, W.S., 2009. Interhemispheric Atlantic seesaw response during the last deglaciation. Nature 457, 1097–1102.

Bassinot, F.C., Marzin, C., Braconnot, P., Marti, O., Mathien-Blard, E., Lombard, F., Bopp, L., 2011. Holocene evolution of summer winds and marine productivity in the tropical Indian Ocean in response to insolation forcing: data-model comparison. Clim. Past 7, 815–829.

Bauska, T.K., Baggenstos, D., Brook, E.J., Mix, A.C., Marcott, S.A., Petrenko, V.V., Schaefer, H., Severinghaus, J.P., Lee, J.E., 2016. Carbon isotopes characterize rapid changes in atmospheric carbon dioxide during the last deglaciation. Proc. Natl. Acad. Sci. http://dx.doi.org/10.1073/pnas.1513868113.

Bond, G., Showers, W., Cheseby, M., Lotti, R., Almasi, P., deMenocal, P., Priore, P., Cullen, H., Hajdas, I., Bonani, G., 1997. A pervasive millennial-scale cycle in North Atlantic Holocene and glacial climates. Science 278, 1257–1266.

Broccoli, A.J., Dahl, K.A., Stouffer, R.J., 2006. Response of the ITCZ to northern hemisphere cooling. Geophys. Res. Lett. 33, L01702. http://dx.doi.org/10.1029/2005GL024546.

Brovkin, V., Ganopolski, A., Archer, D., Munhoven, G., 2012. Glacial CO2 cycle as a succession of key physical and biogeochemical processes. Clim. Past 8, 251–264.

Calvert, S.E., Pedersen, T.F., Naidu, P.D., von Stackelberg, U., 1995. On the organic carbon maximum on the continental slope of the eastern Arabian Sea. J. Mar. Res. 53, 269–296.

Canfield, D.E., 1994. Factors influencing organic carbon preservation in marine sediments. Chem. Geol. 114, 315–329.

Cayre, O., Bard, E., 1999. Planktonic foraminiferal and alkenone records of the last deglaciation from the eastern Arabian Sea. Quat. Res. 52, 337–342.

Cayre, O., Beaufort, L., Vincent, E., 1999. Paleoproductivity in the equatorial Indian Ocean for the last 260,000 yr: a transfer function based on planktonic foraminifera. Quat. Sci. Rev. 18, 839–857.

Chauhan, O.S., Raghavan, B.R., Singh, K., Rajawat, A.S., Ajai, Kader, U.S.A., Nayak, S., 2011. Influence of orographically enhanced SW monsoon flux on coastal processes along the SE Arabian Sea. J. Geophys. Res. 116, C12037. http://dx.doi.org/10.1029/2011JC007454.

Cheng, H., Edwards, R.L., Broecker, W.S., Denton, G.H., Kong, X., Wang, Y., Zhang, R., Wang, X., 2009. Ice age terminations. Science 326, 248–252.

Christensen, J.H., Hewitson, B., Busuioc, A., Chen, A., Gao, X., Held, I., Jones, R., Kolli, R.K., Kwon, W.-T., Laprise, R., Magaña Rueda, V., Mearns, L., Menéndez, C.G., Räisänen, J., Rinke, A., Sarr, A., Whetton, P., 2007. Regional climate projections. In: Solomon, S., Qin, D., Manning, M., Chen, Z., Marquis, M., Averyt, K.B., Tignor, M., Miller, H.L. (Eds.), Climate Change 2007: The Physical Science Basis. Contribution of Working Group I to the Fourth Assessment Report of the Intergovernmental Panel on Climate Change. Cambridge University Press, Cambridge, United Kingdom and New York, NY, USA.

Conan, S.M.-H., Brummer, G.-J.A., 2000. Fluxes of planktic foraminifera in response to monsoonal upwelling on the Somalia Basin margin. Deep-Sea Res. 47, 2207–2227.

Conan, S.M.-H., Ivanova, E.M., Brummer, G.-J.A., 2002. Quantifying carbonate dissolution and calibration of foraminiferal dissolution indices in the Somali Basin. Mar. Geol. 182, 325–349.

Cullen, J.L., Prell, W.L., 1984. Planktonic foraminifera of the northern Indian Ocean: distribution and preservation in surface sediments. Mar. Micropaleontol. 9, 1–52.

Costa, K.M., McManus, J.F., Anderson, R.F., Ren, H., Sigman, D.M., Winckler, G., Fleisher, M.Q., Marcantonio, F., Ravelo, A.C., 2016. No iron fertilization in the equatorial Pacific Ocean during the last ice age. Nature 529, 519–522.

Dahl, K.A., Oppo, D.W., 2006. Sea surface temperature pattern reconstructions in the Arabian Sea. Paleoceanography 21, PA1014. http://dx.doi.org/10.1029/2005PA001162.

Gupta, A.K., Anderson, D.M., Overpeck, J.T., 2003. Abrupt changes in the Holocene Asian southwest monsoon and their links to the north Atlantic Ocean. Nature 421, 354–357.

Gupta, A.K., Raj, M.S., Mohan, K., De, S., 2008. A major change in monsoon-driven productivity in the tropical Indian Ocean during ca 1.2–0.9 Myr: foraminiferal faunal and stable isotope data. Palaeogeogr. Palaeoclimatol. Palaeoecol. 261, 234–245.

Gupta, A.K., Mohan, K., Sarkar, S., Clemens, S.C., Ravindra, R., Uttam, R.K., 2011. East–west similarities and differences in the surface and deep northern Arabian Sea records during the past 21 Kyrs. Palaeogeogr. Palaeoclimatol. Palaeoecol. 301, 75–85.

Guptha, M.V.S., Naidu, P.D., Haake, B.G., Schiebel, R., 2005. Carbonate and carbon fluctuations in the eastern Arabian Sea over 140 ka: implications on productivity changes? Deep-Sea Res. 52, 1981–1993.

Hashimi, N.H., Nigam, R., Nair, R.R., Rajagopalan, G., 1995. Holocene sea level fluctuations on western Indian continental margin: an update. J. Geol. Soc. India 46, 157–162.

Heinrich, H., 1988. Origin and consequences of cyclic ice rafting in the northeast Atlantic Ocean during the past 130,000 years. Quat. Res. 29, 142–152.

Ivanochko, T.S., 2004. Sub-orbital scale variations in the intensity of the Arabian Sea monsoon. Ph.D. Thesis. University of Edinburgh (229p).

Ivanova, E., Schiebel, R., Singh, A.D., Schmiedl, G., Niebler, H.-S., Hemleben, C., 2003. Primary production in the Arabian Sea during the last 135,000 years. Palaeogeogr. Palaeoclimatol. Palaeoecol. 197, 61–82.

Jaccard, S.L., Hayes, C.T., Martínez-García, A., Hodell, D.A., Anderson, R.F., Sigman, D.M., Haug, G.H., 2013. Two modes of change in Southern Ocean productivity over the past million years. Science 339, 1419–1423.

Jaccard, S.L., Galbraith, E.D., Martínez-García, A., Anderson, R.F., 2016. Covariation of deep Southern Ocean oxygenation and atmospheric CO2 through the last ice age. Nature http://dx.doi.org/10.1038/nature16514.

Kessarkar, P.M., Rao, V.P., 2007. Organic carbon in sediments of the southwestern margin of India: influence of productivity and monsoon variability during the late Quaternary. J. Geol. Soc. India 69, 42–52.

Kessarkar, P.M., Rao, V.P., Naqvi, S.W.A., Chivas, A.R., Saino, T., 2010. Fluctuations in productivity and denitrification in the southeastern Arabian Sea during the late Quaternary. Curr. Sci. 99, 485–491.

Kessarkar, P.M., Rao, V.P., Naqvi, S.W.A., Karapurkar, S.G., 2013. Variation in the Indian summer monsoon intensity during the Bølling-A° llerød and Holocene. Paleoceanography 28. http://dx.doi.org/10.1002/palo.20040.

Kohfeld, K.E., Le Quere, C., Harrison, S.P., Anderson, R.F., 2005. Role of marine biology in glacial-interglacial CO2 cycles. Science 308, 74–78.

Lévy, M., Shankar, D., André, J.-M., Shenoi, S.S.C., Durand, F., de Boyer Montégut, C., 2007. Basin-wide seasonal evolution of the Indian Ocean's phytoplankton blooms. J. Geophys. Res. 112, C12014. http://dx.doi.org/10.1029/2007JC004090.

Madhupratap, M., Prasanna Kumar, M.S., Bhattathiri, P.M.A., Dileep Kumar, M., Raghukumar, S., Nair, K.K.C., Ramaiah, N., 1996. Mechanism of the biological response to winter cooling in the northeastern Arabian Sea. Nature 384, 549–552.

Mahesh, B.S., Banakar, V.K., 2014. Change in the intensity of low-salinity water inflow from the bay of Bengal into the eastern Arabian Sea from the last glacial maximum to the Holocene: implications for monsoon variations. Palaeogeogr. Palaeoclimatol. Palaeoecol. 397, 31–37.

Marcott, S.A., Bauska, T.K., Buizert, C., Steig, E.J., Rosen, J.L., Cuffey, K.M., Fudge, T.J., Severinghaus, J.P., Ahn, J., Kalk, M.L., McConnell, J.R., Sowers, T., Taylor, K.C., White, J.W.C., Brook, E.J., 2014. Centennial-scale changes in the global carbon cycle during the last deglaciation. Nature 514, 616–619.

Marra, J., Barber, R.T., 2005. Primary productivity in the Arabian Sea: a synthesis of JGOFS data. Prog. Oceanogr. 65, 159–175.

Martin, J.H., 1990. Glacial-interglacial CO2 change: the iron hypothesis. Paleoceanography 5, 1–13.

Martínez-Garcia, A., Rosell-Melé, A., Geibert, W., Gersonde, R., Masqué, P., Gaspari, V., Barbante, C., 2009. Links between iron supply, marine productivity, sea surface temperature, and CO2 over the last 1.1 Ma. Paleoceanography 24, PA1207. http://dx.doi.org/10.1029/2008PA001657.

Martinson, D.G., Pisias, N.G., Hays, J.D., Imbrie, J., Moore, T.C., Shackleton, N.J., 1987. Age dating and the orbital theory of the ice ages: development of a high-resolution 0 to 300,000-year chronostratigraphy. Quat. Res. 27, 1–29.

Mazumder, A., Nigam, R., 2014. Bathymetric preference of four major genera of rectilinear benthic foraminifera within oxygen minimum zone in Arabian Sea off central west coast of India. J. Earth Syst. Sci. 123, 633–639.

Monnin, E., Indermühle, A., Dallenbach, A., Fluckiger, J., Stauffer, B., Stocker, T.F., Raynaud, D., Barnola, J.-M., 2001. Atmospheric CO2 concentrations over the last glacial termination. Science 291, 112–114.

Naidu, P.D., Malmgren, B.A., 1996. A high-resolution record of late Quaternary upwelling along the Oman margin, Arabian Sea based on planktonic foraminifera. Paleoceanography 11, 129–140.

Naidu, P.D., Prakash Babu, C., Rao, C.M., 1992. The upwelling record in the sediments of the western continental margin of India. Deep-Sea Res. 39, 715–723.

Naidu, P.D., Ramesh Kumar, M.R., Ramesh Babu, V., 1999. Time and space variations of monsoonal upwelling along the west and east coast of India. Cont. Shelf Res. 19, 559–572.

Naidu, P.D., Singh, A.D., Ganeshram, R., Bharti, S.K., 2014. Abrupt climate-induced changes in carbonate burial in the Arabian Sea: causes and consequences. Geochem. Geophys. Geosyst. 15, 1398–1406.

Naik, S.S., Godad, S.P., Naidu, P.D., Tiwari, M., Paropkari, A.L., 2014. Early- to late-Holocene contrast in productivity, OMZ intensity and calcite dissolution in the eastern Arabian Sea. The Holocene 24, 749–755.

Nair, R.R., Ittekkot, V., Manganini, S.J., Ramaswamy, V., Haake, B., Degens, E.T., 1989. Increased particle flux to the deep ocean related to monsoons. Nature 338, 749–751.

Narayana, A.C., Naidu, P.D., Shinu, N., Nagabhushanam, P., Sukhija, B.S., 2009. Carbonate and organic carbon content changes over last 20 ka in the southeastern Arabian Sea: paleoceanographic implications. Quat. Int. 206, 72–77.

Naqvi, S.W.A., 1991. Geographical extent of denitrification in the Arabian Sea in relation to some physical processes. Oceanol. Acta 14, 281–290.

Naqvi, S.W.A., Naik, H., Narvekar, P.V., 2003. The Arabian Sea. In: Black, K., Shimmield, G.B. (Eds.), Biogeochemistry of Marine Systems, pp. 157–207 (Oxford, UK).

Nigam, R., Khare, N., Borole, D.V., 1992. Can benthic foraminiferal morpho-groups be used as indicators of paleomonsoonal precipitation? Estuar. Coast. Shelf Sci. 34, 533–542.

Nigam, R., Mazumder, A., Henriques, P.J., Saraswat, R., 2007. Benthic foraminifera as proxy for oxygen-depleted conditions off the central west coast of India. J. Geol. Soc. India 70, 1047–1054.

Nigam, R., Prasad, V., Saraswat, R., Garg, R., Mazumder, A., Henriques, P.J., 2009. Late Holocene changes in hypoxia off the west coast of India: micropaleontological evidences. Curr. Sci. 96, 708–713.

Pattan, J.N., Masuzawa, T., Yamamoto, M., 2005. Variations in terrigenous sediment discharge in a sediment core from southeastern Arabian Sea during the last 140 ka. Curr. Sci. 89, 1421–1425.

Prasanna Kumar, S., Muraleedharan, P.M., Prasad, T.G., Gauns, M., Ramaiah, N., DeSousa, S.N., Sardessai, S., Madhupratap, M., 2002. Why is the Bay of Bengal less productive during summer monsoon compared to the Arabian Sea? Geophys. Res. Lett. 29, 88.1–88.4.

Prasanna Kumar, S., Narvekar, J., Kumar, A., Shaji, C., Anand, P., Sabu, P., Rejomon, G., Jacob, J., Jayaraj, K.A., Radhika, A., Nair, K.K.C., 2004. Intrusion of the Bay of Bengal water into the Arabian Sea during winter monsoon and associated chemical and biological response. Geophys. Res. Lett. 31, L15304.

Prell, W.L., Kutzbach, J.E., 1987. Monsoon variability over the past 150,000 years. J. Geophys. Res. 92, 8411–8425.

Raza, T., Ahmad, S.M., 2013. Surface and deep water variations in the northeast Indian Ocean during 34–6 ka BP: evidence from carbon and oxygen isotopes of fossil foraminifera. Quat. Int. 298, 37–44.

Reimer, P.J., Baillie, M.G.L., Bard, E., Bayliss, A., Beck, J.W., Blackwell, P.G., Ramsey, C.B., Buck, C.E., Burr, G.S., Edwards, R.L., Friedrich, M., Grootes, P.M., Guilderson, T.P., Hajdas, I., Heaton, T.J., Hogg, A.G., Hughen, K.A., Kaiser, K.F., Kromer, B., McCormac, F.G., Manning, S.W., Reimer, R.W., Richards, D.A., Southon, J.R., Talamo, S., Turney, C.S.M., van der Plicht, J., Weyhenmeyer, C.E., 2009. Intcal09 and Marine09 radiocarbon age calibration curves, 0–50,000 years cal BP. Radiocarbon 51, 1111–1150.

Saraswat, R., Nigam, R., Barreto, L., 2005. Paleoceanographic implications of abundance and mean proloculus diameter of benthic foraminiferal species *Epistominella exigua* in sub-surface sediments from distal Bay of Bengal Fan. J. Earth Syst. Sci. 114, 453–458.

Saraswat, R., Nigam, R., Mackensen, A., Weldeab, S., 2012. Linkage between seasonal insolation gradient in the tropical northern hemisphere and the sea surface salinity of the equatorial Indian Ocean during the last glacial period. Acta Geol. Sin. 86, 801–811.

Saraswat, R., Lea, D.W., Nigam, R., Mackensen, A., Naik, D.K., 2013. Deglaciation in the tropical Indian Ocean driven by interplay between the regional monsoon and global teleconnections. Earth Planet. Sci. Lett. 375, 166–175.

Saraswat, R., Nigam, R., Correge, T., 2014. A glimpse of the Quaternary monsoon history from India and adjoining seas. Palaeogeogr. Palaeoclimatol. Palaeoecol. 397, 1–6.

Sarkar, A., Ramesh, R., Bhattacharya, S.K., Rajagopalan, G., 1990. Oxygen isotope evidence for a stronger winter monsoon current during the last glaciation. Nature 343, 549–551.

Sarkar, A., Bhattacharya, S.K., Sarin, M.M., 1993. Geochemical evidence for anoxic deep water in the Arabian Sea during the last glaciation. Geochim. Cosmochim. Acta 51, 1009–1016.

Schmitt, J., Schneider, R., Elsig, J., Leuenberger, D., Lourantou, A., Chappellaz, J., Köhler, P., Joos, F., Stocker, T.F., Leuenberger, M., Fischer, H., 2012. Carbon isotope constraints on the deglacial CO_2 rise from ice cores. Science 336, 711–714.

Shackleton, N.J., 2000. The 100,000-year ice-age cycle identified and found to lag temperature, carbon dioxide, and orbital eccentricity. Science 289, 1897–1902.

Shankar, D., Shetye, S.R., 1997. On the dynamics of the Lakshadweep high and low in the southeastern Arabian Sea. J. Geophys. Res. 102 (12), 551–12,562.

Shankar, D., Vinayachandran, P.N., Unnikrishnan, A.S., 2002. The monsoon currents in the north Indian Ocean. Prog. Oceanogr. 52, 63–120.

Shankar, D., Gopalakrishna, V.V., Shenoi, S.S.C., Durand, F., Shetye, S.R., Rajan, C.K., Johnson, Z., Araligidad, N., Michael, G.S., 2004. Observational evidence for westward propagation of temperature inversions in the southeastern Arabian Sea. Geophys. Res. Lett. 31, L08305. http://dx.doi.org/10.1029/2004GL019652.

Shakun, J.D., Clark, P.U., He, F., Marcott, S.A., Mix, A.C., Liu, Z., Otto-Bliesner, B., Schmittner, A., Bard, E., 2012. Global warming preceded by increasing carbon dioxide concentrations during the last deglaciation. Nature 484, 49–54.

Shenoi, S.S.C., Shankar, D., Shetye, S.R., 1999. The sea surface temperature high in the Lakshadweep Sea before the onset of the southwest monsoon. J. Geophys. Res. 104, 703–712.

Siddall, M., Rohling, E.J., Almogi-Labin, A., Hemleben, C., Meischner, D., Schmelzer, I., Smeed, D.A., 2003. Sea-level fluctuations during the last glacial cycle. Nature 423, 853–858.

Singh, A.D., Kroon, D., Ganeshram, R., 2006. Millennial scale variations in productivity and OMZ intensity in the eastern Arabian Sea. J. Geol. Soc. India 68, 369–377.

Singh, A.D., Jung, S.J.A., Darling, K., Ganeshram, R., Ivanochko, T., Kroon, D., 2011. Productivity collapses in the Arabian Sea during glacial cold phases. Paleoceanography 26, PA3210. http://dx.doi.org/10.1029/2009PA001923.

Singh, A.D., Rai, A.K., Verma, K., Das, S., Bharti, S.K., 2015. Benthic foraminiferal diversity response to the climate induced changes in the eastern Arabian Sea oxygen minimum zone during the last 30 ka BP. Quat. Int. 374, 118–125.

Sirocko, F., Sarnthein, M., Erlenkeusers, H., Lange, H., Arnold, M., Duplessy, J.C., 1993. Century scale events in monsoonal climate over the past 24,000 years. Nature 364, 322–324.

Sirocko, F., 2002. Sedimentology on core MD77-191 http://dx.doi.org/10.1594/PANGAEA.77650.

Sirocko, F., Schonberg, D.G., Devey, C., 2000. Processes controlling trace element geochemistry of Arabian Sea sediments during the last 25,000 years. Glob. Planet. Chang. 26, 217–303.

Smitha, B.R., Sanjeevan, V.N., Vimalkumar, K.G., Ravichandran, C., 2008. On the upwelling off the southern tip and along the west coast of India. J. Coast. Res. 24, 95–102.

Southon, J., Kashgarian, M., Fontugne, M., Metivier, B., Yim, W.W.-S., 2002. Marine reservoir corrections for the Indian Ocean and southeast Asia. Radiocarbon 44, 167–180.

Southon, J., Noronha, A.L., Cheng, H., Edwards, R.L., Wang, Y., 2012. A high-resolution record of atmospheric ^{14}C based on Hulu Cave speleothem H82. Quat. Sci. Rev. 33, 32–41.

Spero, H.J., Lea, D.W., 2002. The cause of carbon isotope minimum events on glacial terminations. Science 296, 522–525.

Stuiver, M., Reimer, P.J., 1993. Extended ^{14}C database and revised CALIB radiocarbon calibration program. Radiocarbon 35, 215–230.

Tierney, J.E., Pausata, F.S.R., deMenocal, P.B., 2016. Deglacial Indian monsoon failure and north Atlantic stadials linked by Indian Ocean surface cooling. Nat. Geosci. 9, 46–50.

Tiwari, M., Ramesh, R., Somayajulu, B.L.K., Jull, A.J.T., Burr, G.S., 2005. Early deglacial (~19–17 ka) strengthening of the northeast monsoon. Geophys. Res. Lett. 32, L19712. http://dx.doi.org/10.1029/2005GL024070.

Waelbroeck, C., Labeyrie, L., Michel, E., Duplessy, J.C., McManus, J.F., Lambeck, K., Balbon, E., Labracherie, M., 2002. Sea-level and deep water temperature changes derived from benthic foraminifera isotopic records. Quat. Sci. Rev. 21, 295–305.

Watson, A.J., Bakker, D.C.E., Ridgwell, A.J., Boyd, P.W., Law, C.S., 2000. Effect of iron supply on Southern Ocean CO2 uptake and implications for glacial atmospheric CO_2. Nature 407, 730–733.

Wiggert, J.D., Hood, R.R., Banse, K., Kindle, J.C., 2005. Monsoon-driven biogeochemical processes in the Arabian Sea. Prog. Oceanogr. 65, 176–213.

Wyrtki, K., 1973. In: Zeitzschel, B. (Ed.), Physical Oceanography of the Indian Ocean: The Biology of the Indian Ocean. Springer-Verlag, Berlin, pp. 18–36.

Zaric, S., Donner, B., Fischer, G., Mulitza, S., Wefer, G., 2005. Sensitivity of planktic foraminifera to sea surface temperature and export production as derived from sediment trap data. Mar. Micropaleontol. 55, 75–105.